J Fusion Energ
DOI 10.1007/s10894-012-9536-2

ORIGINAL RESEARCH

# Soft X-Ray Emission in the Water Window Region with Nitrogen Filling in a Low Energy Plasma Focus

**M. Akel · S. Lee**

© Springer Science+Business Media, LLC 2012

**Abstract** For operation of the plasma focus in nitrogen, a focus pinch compression temperature range of 74–173 eV ($0.86 \times 10^6$–$2 \times 10^6$ K) is found to be suitable for good yield of nitrogen soft X-rays in the water window region. Using this temperature window, numerical experiments using five phase Lee model have been investigated on UNU/ICTP PFF and APF plasma focus devices with nitrogen filling gas. The Lee model was applied to characterize and optimize these two plasma focus devices. The optimum nitrogen soft X-ray yield was found to be $Y_{sxr} = 2.73$ J, with the corresponding efficiency of 0.13 % for UNU/ICTP PFF device, while for APF device it was $Y_{sxr} = 4.84$ J, with the corresponding efficiency of 0.19 % without changing the capacitor bank, merely by changing the electrode configuration and operating pressure. The Lee model code was also used to run numerical experiments for optimizing soft X-ray yield with reducing $L_0$, varying $z_0$ and 'a'. From these numerical experiments we expect to increase the nitrogen soft X-ray yield of low energy plasma focus devices to maximum value of near 8 J, with the corresponding efficiency of 0.4 %, at an achievable $L_0 = 10$ nH.

M. Akel (✉)
Department of Physics, Atomic Energy Commission,
P. O. Box 6091, Damascus, Syria
e-mail: pscientific@aec.org.sy

S. Lee
Institute for Plasma Focus Studies, 32 Oakpark Drive,
Chadstone, VIC 3148, Australia

S. Lee
INTI International University, 71800 Nilai, Malaysia

**Keywords** UNU/ICTP PFF · Soft X-ray · Nitrogen gas · Lee model

## Introduction

A hot, dense plasma can be generated by imploding and compressing a cylindrical plasma or multiple parallel wires by means of a magnetic field. Usually an azimuthal magnetic field is generated by currents of several hundred kilo amps up to a few mega amps driven through the plasma by a fast capacitor bank. During implosion, electrical energy is converted into kinetic energy of the moving plasma and into thermal energy in the plasma. The hot pinch plasma is formed when the plasma stagnates on axis and exists for typically tens of nanoseconds for kJ devices. The pinch plasma energy is additionally increased by compression due to the pinch effect and by joule heating. During its lifetime the pinch plasma is ionized to higher ionization states and efficiently converts a large amount of its energy into soft X-radiation. In pinch plasmas, soft X-ray radiation is generated mainly by radiative recombination and ionic line emission. The emission characteristics of the pinch are determined by the elements used and by several physical plasma parameters and their temporal and spatial variations; for example, the electron density and temperature determine the states of ionization and the excitation rate. The plasma parameters depend on the power fed into the plasma, the load geometry and the imploded mass. Whilst the pinch effect is more or less similar in various schemes used to generate the emitting plasma, the initiation of the discharges differs significantly [1]. The different schemes are known as Z-pinch [2], X-pinch [3], vacuum spark [4, 5] and plasma focus (PF) [6, 7]. The plasma focus is the simplest in construction and yet provides the highest X-ray emission compared to other

Published online: 03 April 2012

devices of equivalent energy [8, 9]. Nitrogen gas has been used widely in plasma focus devices as an emitter of soft X-rays [10–14], and plasma focus devices operated with pure nitrogen are developed as sources for X-ray microscopy [1, 15, 16]. X-ray microscopy provides higher resolution than optical microscopy and higher penetration ability than electron microscopy. Moreover, X-ray microscopy allows the imaging of living hydrated biological specimens. The wavelength range between the K-absorption edges of oxygen ($\lambda = 2.34$ nm) and carbon ($\lambda = 4.38$ nm) is especially interesting for this because the radiation in this wavelength range (so called "water window") is weakly absorbed by water but strongly absorbed by organic matter resulting in a good contrast of wet samples. In principle all ionic lines from plasmas emitting at the water window can be used. K-shell lines are advantageous over L- or M-shell lines because of their larger spectral separation. In particular, the first resonant lines, i.e. the ls-2p line and the $ls^2$-1s2p line, for hydrogen-like and helium-like ions, respectively, are most intense because they are of highest oscillator strength within the line series. These lines are located in the water window wavelength range for nitrogen, in which, the shorter wavelength of N VII is close to the oxygen K-edge where transmission losses by absorption in wet specimens are the lowest [1].

Lebert et al. [1], reported that a plasma focus device with 2.5 kJ electrical storage energy and 350 kA peak current has been developed as a source for an X-ray microscopy. Nitrogen gas is used as discharge load to generate the N VII ls-2p and N VI $ls^2$-ls3p lines. The emission is used in the axial direction with respect to the plasma column. The emission spectrum of this source has been recorded with a resolution of $\lambda/\Delta\lambda = 300$. It consists mainly of emission lines and recombination continua of hydrogen-like and helium-like ions. The N VII ls-2p line at 2.478 nm and the N VI $ls^2$-ls3p line at 2.49 nm, coinciding within a reciprocal relative bandwidth of $\lambda/\Delta\lambda = 210$, are resolved.

The Lee model code has been modified to include nitrogen gas and it has been then used to characterize the plasma focus device operated in nitrogen [17]. The suitable temperature range for generating H-like [$Ly_\alpha$ (1 s-2p, $N_2$: 2.478 nm)) and He-like ($He_\beta$ (1 $s^2$-1s3p, $N_2$: 2.496 nm)] ions in nitrogen plasma (therefore X-ray emissions in the water window region) was found to be between 74–173 eV ($0.86 \times 10^6$–$2 \times 10^6$ K) [17].

In the modified Lee model code version RADPF5.15 K, we take the nitrogen soft X-ray yield to be equivalent to line radiation yield i.e. $Y_{sxr} = Q_L$ at the following temperature range 74–173 keV. The detailed description, theory, latest code and a broad range of results of this 'Universal Plasma Focus Laboratory Facility' are available for download from reference [18].

In the present work, the five phase radiative Lee Model has been used to characterize and optimize UNU/ICTP PFF [14, 19] and APF devices [13] for nitrogen soft X-ray yield and to find the optimum combination of ($p_0$, $z_0$ and 'a') and the optimum combination of ($L_0$, $z_0$ and 'a') for the maximum nitrogen soft X-ray yield.

## Numerical Experiments on UNU/ICTP PFF with Nitrogen Filling Gas

To start the numerical experiments, a measured discharge current trace of the UNU/ICTP PFF with nitrogen filling gas, has been taken from the reference [14] (see Fig. 1a). The following bank, tube and operation parameters are used: Bank: static inductance $L_0 = 110$ nH, $C_0 = 30$ μF, stray resistance $r_0 = 12$ mΩ, Tube: cathode radius $b = 3.2$ cm, anode radius $a = 0.95$ cm, anode length $z_0 = 16$ cm, operation: voltage $V_0 = 12$ kV, pressure $p_0 = 1.05$ Torr nitrogen. The computed total discharge

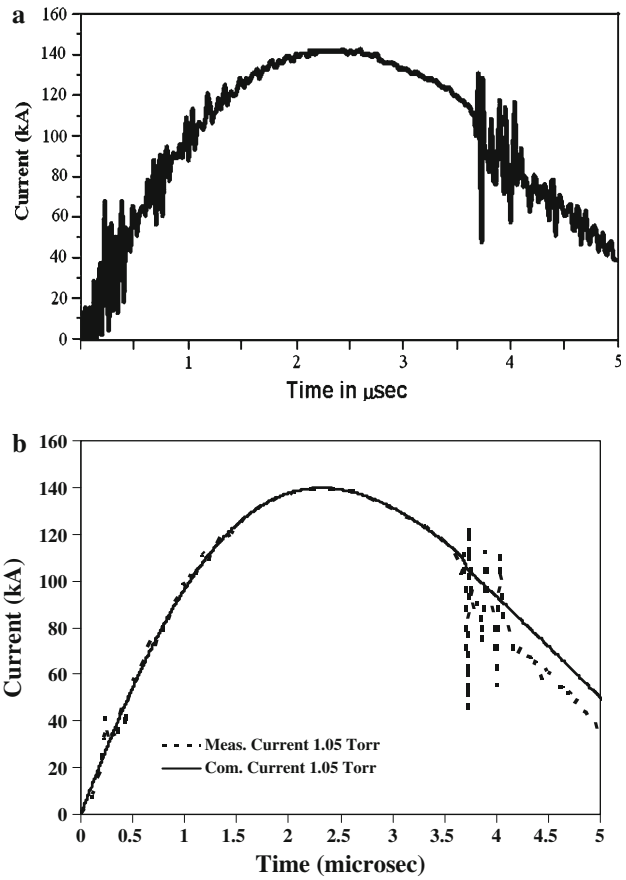


**Fig. 1** a The experimental current trace of the UNU/ICTP PFF at 12 kV, 1.05 Torr at nitrogen filling gas [14]. b Comparison of the experimental current trace (*dotted line*) with the computed one (*solid smooth line*) of the UNU/ICTP PFF at 12 kV, 1.05 Torr at nitrogen filling gas

current waveform is fitted to the measured by varying model parameters $f_m$, $f_c$, $f_{mr}$ and $f_{cr}$ one by one until the computed waveform agrees with the measured waveform (Fig. 1b). First, the axial model factors $f_m$, $f_c$ are fitted until the computed rising slope of the total current trace and the rounding off of the peak current as well as the peak current itself are in reasonable (typically good) fit with the measured total current trace. Then we proceed to adjust (fit) the radial phase model factors $f_{mr}$ and $f_{cr}$ until the computed slope and depth of the dip agree with the measured. In this case, the following fitted model parameters are obtained: $f_m = 0.06$, $f_c = 0.7$, $f_{mr} = 0.15$ and $f_{cr} = 0.7$. These fitted values of the model parameters are then used for the computation of all the discharges at various pressures. The numerical experiments using RADPF5.15 K at the bank and tube parameters last mentioned above and using the fitted model parameters give then the following results: the end axial speed to be $V_a = 5.74$ cm/μs, the speed factor ($SF = (I_0/ap_0^{1/2})$ is 144 kA/cm per [Torr of nitrogen]$^{1/2}$ [20].

The plasma parameters (dimensions, speeds and line radiation) are changing slowly in the first half part of the inward shock phase. The final plasma column is 0.097 cm in radius, and 1.35 cm in length. The inward shock speed is steadily increasing in the inward shock phase to a final on-axis speed of $V_s = 19.8$ cm/μs and the radial piston speed is also increasing to a maximum value of $V_p = 14$ cm/μs and the pinch duration is about 11.2 ns. At these experimental conditions was found that soft X-ray emitted from nitrogen plasma focus to be 0.033 J. The peak values of total discharge current $I_{peak}$ is about 140 kA, the pinch current $I_{pinch}$ is 74 kA, and the focusing time at about 3.75 μs. The focusing time increases with increase in the gas pressure, while it decreases with increase in the charging voltage. This can be ascribed to the increase in energy pumping to plasma focus which causing an increase in the current sheath velocity in both axial and radial phases before forming focus. These fitted values of the model parameters are then used for the computation of all the discharges at various pressures, fixing all the mentioned above parameters. This procedure of fixing the model parameters is reasonable in view of recent experimental work on two different machines in different gases operated over a range of pressures [21]. The pressure was varied from 0.2 to 2.2 Torr. From obtained results, it is seen that the $Y_{sxr}$ increases with increasing pressure until it reaches the maximum value about 0.14 J at $p_0 = 1.55$ Torr, after which it decreases with higher pressures. As expected as $p_0$ is increased, the end axial speed, the inward shock speed and the radial piston speed all reduced. The decrease in speeds lead to lowering of plasma temperatures below that needed for soft X-ray production (see Fig. 2). We note that a shift of operating pressure to 1.55 Torr would increase the computed $Y_{sxr}$ to 0.14 J at $V_a = 4.5$ cm/μs with the corresponding efficiency is about 0.0066 %. The peak value of

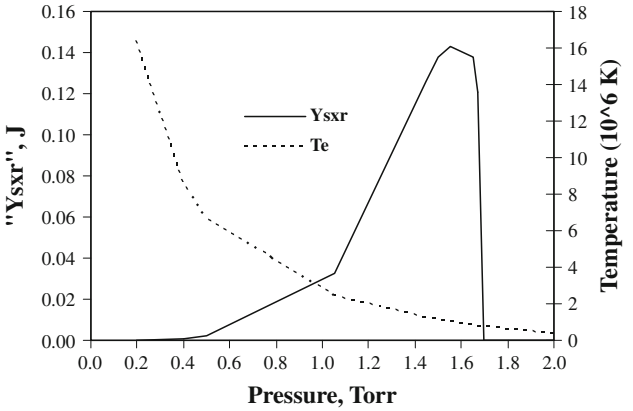


**Fig. 2** The soft X-ray yield, the plasma temperatures as functions of the pressure from UNU/ICTP PFF

total discharge current $I_{peak}$ slightly decreases with decreasing pressure. This is due to increasing dynamic resistance (rate of change of plasma inductance, dL/dt gives rise to a dynamic resistance equal to 0.5 dL/dt) [22] due to the increasing current sheath speed as pressure is decreased. We note that, on the contrary, the current $I_{pinch}$ that flows through the pinched plasma column increases with decreasing pressure until it reaches the maximum 88 kA at 0.4 Torr. This is due to the shifting of the pinch time closer and closer towards the time of peak current as the current sheet moves faster and faster [23]. As the pressure is decreased, the increase in $I_{pinch}$ may be expected to favour $Y_{sxr}$; however there is a competing effect that decreasing pressure reduces the number density. The interaction of these competing effects will decide on the actual yield versus pressure behavior as shown in the computed results. We next wish to optimize the soft X-ray yield from UNU/ICTP PFF Plasma focus with nitrogen gas, so more numerical experiments were also carried out with the above model parameters; but varying $p_0$, $z_0$ and 'a' keeping c = b/a constant at value c = 3.368. The pressure $p_0$ was varied from 0.1 to 3.5 Torr, using procedures published in references [17, 24, 25].

The numerical experiments showed that $z_0$ needed to be increased to optimize the $Y_{sxr}$. Thus whilst external inductance $L_0$ is fixed at a constant value and an axial section inductance $L_a$ is increased due to increasing the anode length, the pinch inductance $L_p$ is reduced due to decreasing the pinch length (see Fig. 3). The optimized results for each value of $p_0$ presented, that the soft X-ray yield slightly increases with increasing $p_0$ until it reaches a maximum value of 2.73 J at $p_0 = 0.3$ Torr; then the $Y_{sxr}$ decreases with further pressure increase. Figure 4 shows soft X-ray yield as function of $p_0$, with the plasma focus operated at the optimum combination of $z_0$ and 'a' corresponding to each $p_0$. From the numerical experiments for UNU/ICTP PFF with $L_0 = 110$ nH, $C_0 = 30$ μF,

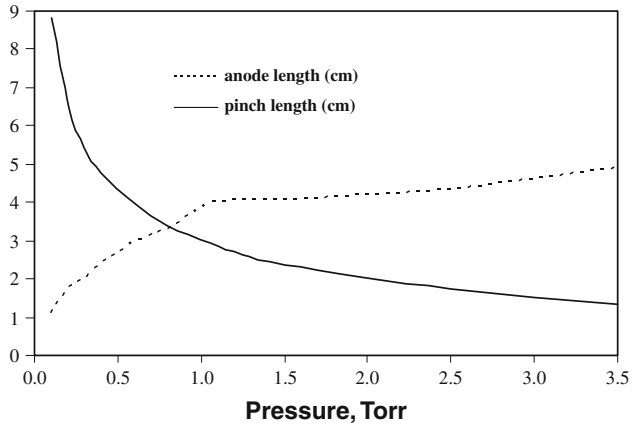


**Fig. 3** Variation of the anode length and pinch length versus pressure in UNU/ICTP PFF

$r_0 = 12$ mΩ, $V_0 = 12$ kV we have thus found the optimum combination of $p_0$, $z_0$ and 'a' for nitrogen $Y_{sxr}$ as 0.3 Torr, 2 and 3.81 cm respectively, with the outer radius b = 12.84 cm. This combination gives $Y_{sxr} = 2.73$ J, with the corresponding efficiency is about 0.13 % and the end axial speed is of 2.32 cm/μs. We also note that at this optimum configuration $I_{peak} = 140$ kA, $I_{pinch} = 89$ kA. Many numerical experiments have been also systematically carried out to optimize the soft X-ray yield from UNU/ICTP PFF with nitrogen gas, varying $L_0$, $z_0$ and 'a' keeping 'c' and RESF constant. The external inductance $L_0$ was varied from 110 nH to 5 nH. These numerical experiments showed that reducing $L_0$ increases the total current from $I_{peak} = 140$ kA at $L_0 = 110$ nH to $I_{peak} = 315$ kA at achievable value incorporating low inductance technology of $L_0 = 10$ nH, the pinch current $I_{pinch}$ reaches a maximum of 170 kA and the soft X-ray yield increases to a maximum value of 10 J, with the corresponding efficiency is about 0.47 %.

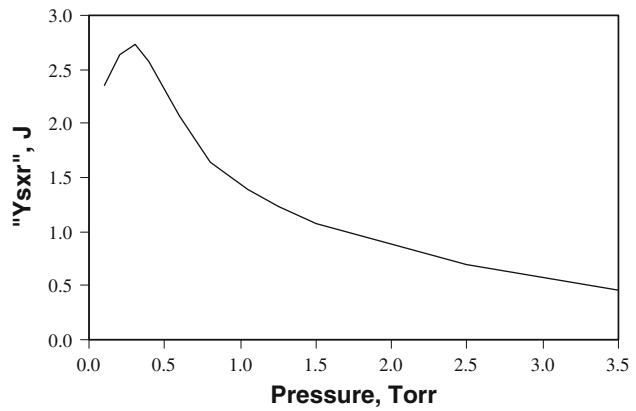


**Fig. 4** The soft X-ray yield from UNU/ICTP PFF as function of pressure, anode length and inner radius ($Y_{sxr}$ vs $p_0$, $z_0$ and 'a')

## Numerical Experiments on APF with Nitrogen Filling Gas

The effect of applied voltage and gas pressure on the focusing time, and X-ray emission (with photon energy more than 1 keV) from nitrogen plasma focus in Amirkabir plasma focus device (APF) have been experimentally investigated [26–28]. Based on recently published discharge current waveforms of APF device with nitrogen filling gas, numerical experiments have been carried out using 5-phase Lee model to characterize and optimize APF device for He-like and H-like ions with nitrogen gas, i. e. for soft X-ray emission in the water window region. For these purposes, a measured discharge current trace of the APF device with nitrogen filling gas has been taken from the references [26–28] (see Fig. 5a). The following bank, tube and operation parameters are used: Bank: static inductance $L_0 = 115$ nH, $C_0 = 36$ μF, stray resistance $r_0 = 8$ mΩ, Tube: cathode radius b = 2.235 cm, anode radius a = 1 cm, anode length $z_0 = 14.8$ cm, Operation: voltage $V_0 = 12$ kV, pressure $p_0 = 3.5$ Torr nitrogen. The computed total discharge current waveform is fitted to the measured by varying model parameters $f_m$, $f_c$, $f_{mr}$ and $f_{cr}$

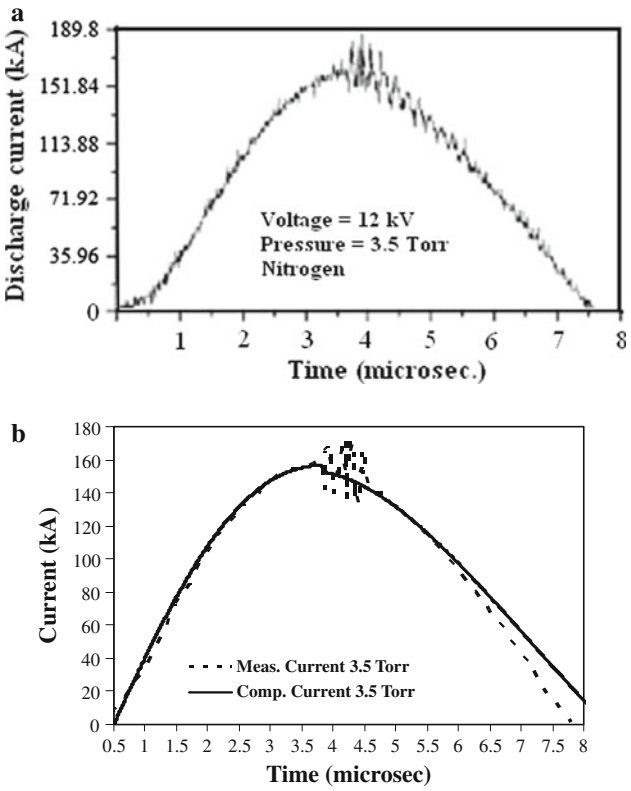


**Fig. 5** a The experimental current trace of the APF at 12 kV, 3.5 Torr at nitrogen filling Gas [27]. b Comparison of the experimental current trace (*dotted line*) with the computed one (*solid smooth line*) of the APF at 12 kV, 3.5 Torr at nitrogen filling gas

one by one until the computed waveform agrees with the measured waveform (Fig. 5b). In this case, the following fitted model parameters are obtained: $f_m = 0.02$, $f_c = 0.7$, $f_{mr} = 0.15$ and $f_{cr} = 0.7$. These fitted values of the model parameters are then used for the computation of all the discharges at various pressures. The numerical experiments using RADPF5.15 K at the bank and tube parameters last mentioned above and using the fitted model parameters give then the following results: the end axial speed to be $V_a = 7.53$ cm/μs, the speed factor ($SF = (I_0/ap_0^{1/2})$ is 84 kA/cm per [Torr of nitrogen]$^{1/2}$. The plasma parameters (dimensions, speeds and line radiation) are changing slowly in the first half part of the inward shock phase. The final plasma column is 0.1 cm in radius, and 1.4 cm in length. The inward shock speed is steadily increasing in the inward shock phase to a final on-axis speed of $V_s = 16$ cm/μs and the radial piston speed is also increasing to a maximum value of $V_p = 11.3$ cm/μs and the pinch duration is about 14 ns. At these experimental conditions was found that soft X-ray emitted from nitrogen plasma focus to be 0.6 J. The peak values of total discharge current $I_{peak}$ is about 157 kA, the pinch current $I_{pinch}$ is 1.7 kA, and the focusing time at about 3.8 μs. These fitted values of the model parameters are then used for the computation of all the discharges at various pressures, fixing all the mentioned above parameters. The pressure was varied from 0.5 to 7 Torr. From obtained results, it is seen that the $Y_{sxr}$ increases with increasing pressure until it reaches the maximum value about 0.6 J at $p_0 = 3.5$ Torr at $V_a = 7.5$ cm/μs with the corresponding efficiency is about 0.023 %, after which it decreases with higher pressures. As expected as $p_0$ is increased, the end axial speed, the inward shock speed and the radial piston speed all reduced. The decrease in speeds lead to lowering of plasma temperatures below that needed for soft X-ray production (see Fig. 6). In addition to that, many numerical experiments have been carried out to study of the effect of applied voltage on soft X-ray emitted from nitrogen plasma focus. In Fig. 7 variation of soft X-ray yields from APF with pressure are plotted at applied voltages of 10, 11, 12, and 13 kV. From this figure, it can be noticed that with increasing applied voltages from 10 to 13 kV, soft X-ray yield from plasma focus increases from 0.4 to 0.7 J. It can also be seen, for all applied voltages, the general features of soft X-ray yields are almost the same. With the increment of pressure, the intensity of soft X-ray is increased to a maximum value and then decreased. X-ray emission increases with the pressure because of increasing in density of the pinched radiating plasma which causes an increase in X-ray yield. However, beyond optimum pressure, emission of X-ray decreases. The reason is that at a higher pressure, the time to pinch exceeds the time to maximum in the discharge current. Also as pressure increases from optimum value, the current

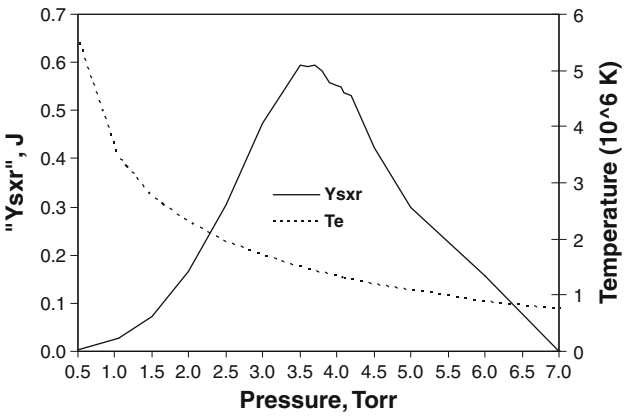


**Fig. 6** The soft X-ray yield, the plasma temperatures as functions of the pressure from APF device

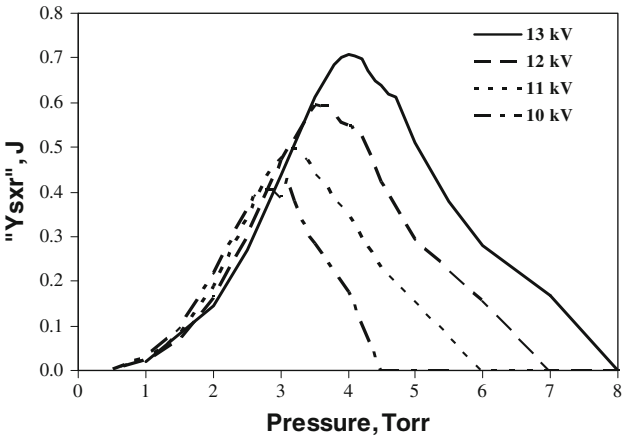


**Fig. 7** Variation of soft X-ray yields from APF with pressure at applied voltages of 10, 11, 12, and 13 kV

sheath at the insulator and also during the rundown phase becomes non-uniform. We next wish to optimize the soft X-ray yield from APF Plasma focus with nitrogen gas, so more numerical experiments were also carried out with the above model parameters; but varying $p_0$, $z_0$ and 'a' keeping $c = b/a$ constant at value $c = 3.368$. The pressure $p_0$ was varied from 0.1 to 5.5 Torr. The numerical experiments showed that $z_0$ also needed to be increased to optimize the $Y_{sxr}$ and the soft X-ray yield slightly increases with increasing $p_0$ until it reaches a maximum value of 4.84 J at $p_0 = 0.2$ Torr; then the $Y_{sxr}$ decreases with further pressure increase (see Fig. 8). From the numerical experiments for APF with $L_0 = 145$ nH, $C_0 = 36$ μF, $r_0 = 8$ mΩ, $V_0 = 12$ kV we have thus found the optimum combination of $p_0$, $z_0$ and 'a' for nitrogen $Y_{sxr}$ as 0.2 Torr, 6.28 and 5.25 cm respectively, with the outer radius $b = 11.72$ cm This combination gives $Y_{sxr} = 4.84$ J, with the corresponding efficiency is about 0.19 % and the end axial speed is of 5.1 cm/μs. We also note that at this optimum

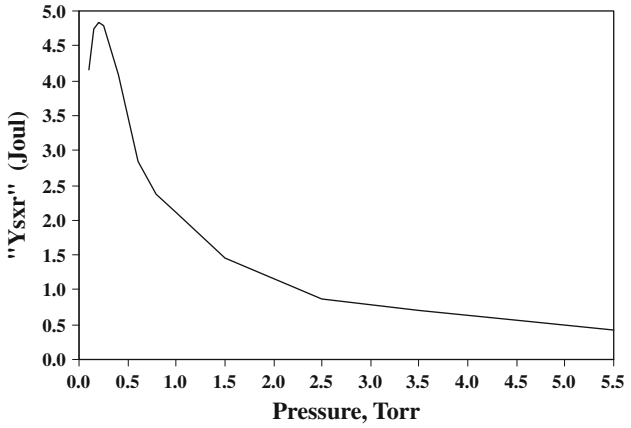


**Fig. 8** The soft X-ray yield from APF as function of pressure, anode length and inner radius ($Y_{sxr}$ vs $p_0$, $z_0$ and 'a')

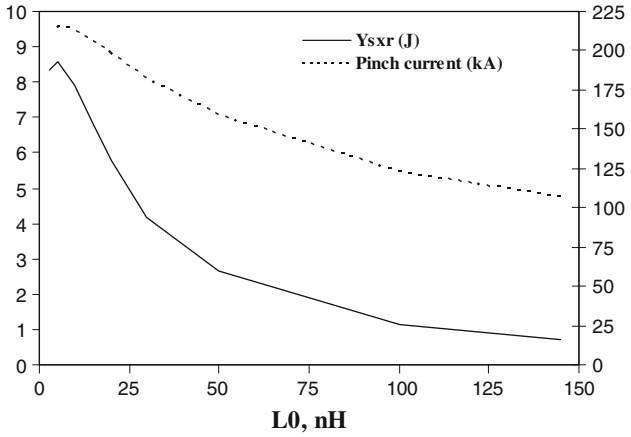


**Fig. 9** Variation of the soft X-ray yield and pinch current from APF as function of Inductance, anode length and inner radius ($Y_{sxr}$ vs $L_0$, $z_0$ and 'a')

configuration $I_{peak} = 154$ kA, $I_{pinch} = 100$ kA. The influence of $L_0$ reduction on the total current traces using RADPF5.15 K was investigated. At each $L_0$, after $z_0$ was varied, the inner radius 'a' was adjusted to obtain the optimum X-ray yield, which corresponds closely to the largest $I_{pinch}$. The soft X-ray optimization for each value of $L_0$, varying $z_0$ and 'a' is shown in Table 1. The table shows that as $L_0$ is reduced, $I_{peak}$ increases with each reduction in $L_0$ with no sign of any limitation as function of $L_0$. However, $I_{pinch}$ reaches a maximum of 216 kA at $L_0 = 5$ nH, then it decreases with each reduction in $L_0$. Thus $I_{peak}$ doesn't show any limitation as $L_0$ is progressively reduced. However $I_{pinch}$ has a maximum value. This pinch current limitation effect is not a simple, but it is a combination of the two complex effects: the interplay of the various inductances involved in the plasma focus processes abetted by the increasing coupling of $C_0$ to the inductive energetic processes, $L_0$ is reduced. From Table 1 it can be seen, that as $L_0$ decreased, the soft X-ray yield increases until it reaches a maximum value of 8.58 J at $L_0 = 5$ nH, with the corresponding efficiency is about 0.33 %; beyond which the soft X-ray yield and the corresponding efficiency do not increase with reducing $L_0$ (see Fig. 9). Thus with decreasing $L_0$ the pinch current $I_{pinch}$ and the soft X-ray yield show limitation. The obtained results confirm the pinch current limitation effect in argon plasma focus, and consequently the soft X-ray yield. Looking at Table 1, it is noticed that as $L_0$ was progressively reduced, to optimize 'a' had to be progressively increased and $z_0$ progressively decreased. Based on the obtained results of these sets of numerical experiments on APF with nitrogen gas, we can say that to improve the soft X-ray yield, $L_0$ should be reduced to a value around 10–15 nH (which is an achievable range incorporating low inductance technology, below which the pinch current $I_{pinch}$ and the soft X-ray yield $Y_{sxr}$ would not be improved much, if at all. These experiments confirm the pinch current limitation effect [29], and consequently the soft X-ray yield for the argon plasma focus. Finally, we would like to emphasize that we, practically, have no intention (or ambition) to go below 10–15 nH (which is an achievable range), but in our numerical

**Table 1** For each $L_0$ the optimization combination of $z_0$ and 'a' were found and are listed here. Bank parameters: $L_0 = 145$ nH, $C_0 = 36$ μF, $r_0 = 8$ mΩ, $V_0 = 12$ kV, $c = b/a = 2.235$, RESF = 0.126, $f_m = 0.02$, $f_c = 0.7$, $f_{mr} = 0.15$, $f_{cr} = 0.7$. Operating at 3.5 Torr nitrogen gas, $V_0 = 12$ kV

| $L_0$ (nH) | $z_0$ (cm) | a (cm) | b (cm) | $I_{peak}$ (kA) | $I_{pinch}$ (kA) | $a_{min}$ (cm) | $Z_{max}$ (cm) | $V_a$ (cm/μs) | $Y_{sxr}$ (J) | $I_{peak}$/a (kA/cm) |
|---|---|---|---|---|---|---|---|---|---|---|
| 145 | 13.5 | 1.10 | 2.46 | 157.7 | 107.6 | 0.11 | 1.5 | 6.9 | 0.69 | 143.4 |
| 100 | 13.0 | 1.25 | 2.79 | 186.0 | 123.8 | 0.12 | 1.7 | 7.3 | 1.12 | 148.8 |
| 50 | 7.0 | 1.60 | 3.58 | 248.8 | 160.0 | 0.16 | 2.3 | 7.3 | 2.68 | 155.5 |
| 30 | 6.0 | 1.70 | 3.80 | 300.8 | 183.8 | 0.18 | 2.4 | 8.3 | 4.18 | 176.9 |
| 20 | 5.0 | 1.90 | 4.25 | 350.1 | 199.1 | 0.22 | 2.8 | 8.6 | 5.78 | 184.3 |
| 15 | 4.0 | 2.00 | 4.47 | 382.7 | 207.1 | 0.24 | 2.9 | 8.8 | 6.81 | 191.3 |
| 10 | 3.5 | 2.10 | 4.69 | 432.7 | 214.2 | 0.28 | 3.1 | 9.5 | 7.91 | 206.1 |
| 5 | 2.5 | 2.20 | 4.92 | 510.7 | 216.0 | 0.34 | 3.3 | 10.7 | 8.58 | 232.2 |
| 3 | 2.3 | 2.20 | 4.91 | 559.2 | 212.8 | 0.36 | 3.3 | 12.0 | 8.32 | 254.3 |

experiments using RADPF5.15 K we go down to a low values of $L_0$ (5–3 nH) just to find the pinch current limitation effect.

## Conclusions

The Lee model code was applied to characterize the UNU/ICTP PFF and APF Plasma Focus devices, finding a maximium nitrogen soft X-ray yield in the water window region of 2.73 J, with the corresponding efficiency of 0.13 % for UNU/ICTP PFF, while for APF device it was found to be $Y_{sxr} = 4.84$ J, with the corresponding efficiency of 0.19 %. The effect of external inductance $L_0$ has been studied and numerical experiments show that, with reducing $L_0$, the nitrogen soft X-ray yield of low energy plasma focus increases up to 8 J with efficiency $\sim$0.4 %.

**Acknowledgments** The authors would like to thank Director General of AECS, for encouragement and permanent support. They would also like to express thanks to Mrs. Sheren Isamael, who collaborated going through all the numerical experiments using Lee Model.

## References

1. R. Lebert, D. Rothweiler, A. Engel, K. Bergmann, W. Neff, Opt. Quant. Electron. **28**, 241–259 (1996)
2. V.L. Kantsyrev et al., in *Proceedings 3rd International Conference on Dense Z-pinches*, vol. 299, ed. by M. Haines, A. Knight (New York: AIP, 1993), p. 226
3. D.A. Hammer et al., Appl. Phys. Lett. **57**, 2083 (1990)
4. A. Ikhlef et al., in *Proceedings 3rd International Conference on Dense Z-pinches,*, vol. 299, ed. by M. Haines, A. Knight (New York: AIP, 1993), p. 218
5. C.S. Wong, S. Lee, Rev. Sci. Instrum. **55**, 1125 (1984)
6. J.W. Mather, Phys. Fluids **8**, 366 (1965)
7. M. Zakaullah et al., Phys. Plasmas **6**, 3188 (1999)
8. M. Zakaullah et al., Appl. Phys. Lett. **78**, 877 (2001)
9. S. Lee et al., IEEE Trans. Plasma Sci. **26**, 1119 (1998)
10. M. Shafiq et al., Mod. Phys. Lett. B **16**(9), 309 (2002)
11. M. Shafiq, et al., J. Fusion Energ. 20(3) 113, September 2001 (q 2002)
12. N.K. Neog et al., J. Appl. Phys. **99**, 013302 (2006)
13. A. Roomi et al., J. Fusion Energ. doi:10.1007/s10894-011-9395-2, (2011)
14. M.A.I. Elgarhy, M.Sc. Thesis, Plasma Focus and its Applications, Cairo (2010)
15. F. Richer, et al., Dense z-pinches in *Proceedings of the Second International Conference* (New York/N.Y.: AIP, 1989), p. 195
16. R. Lebert, A. Engel, W. Neff, J. Appl. Phys. **78**(11), 6414–6420 (1995)
17. M. Akel, S. Al-Hawat, S. Lee, J. Fusion Energ. **28**(4), 355–363 (2009)
18. S. Lee. "Radiative Dense Plasma Focus Computation Package: RADPF", http://www.intimal.edu.my/school/fas/UFLF/. http://www.plasmafocus.net/IPFS/modelpackage/File1RADPF.htm .(October 2011)
19. S. Lee et al., Am. J. Phys. USA. 56:62–68 (1988)
20. S. Lee, A. Serban, IEEE Trans. Plasma Sci. **24**, 1101–1105 (1996)
21. Sh. Al-Hawat, M. Akel, S. Lee, S.H. Saw, J. Fusion Energ. **31**, 13–20 (2012)
22. S. Lee, Appl. Phys. Lett. **95**(15), 151503 (2009)
23. S.H. Saw et al., IEEE Trans. Plasma Sci. **37**(7), 1276–1282 (2009)
24. S. Lee, S.H. Saw, P. Lee, R.S. Rawat, Plasma Phys. Controlled Fusion. 51:105013, (pp. 8) (2009)
25. M. Akel, Sh. Al-Hawat, S.H. Saw, S. Lee, J. Fusion Energ. **29**(3), 223–231 (2010)
26. A. Roomi et al., J. Fusion Energ. (2011). doi:10.1007/s10894-011-9388-1
27. A. Roomi et al., J. Fusion Energ. (2011). doi:10.1007/s10894-011-9464-6
28. A. Roomi et al., J. Fusion Energ. (2011). doi:10.1007/s10894-011-9501-5
29. S. Lee, S.H. Saw, Appl. Phys. Lett. **92**, 021503 (2008)